Luminescence and thermoluminescence of $Sr_2B_5O_9X:Ce^{3+},A^+$ (X = Cl, Br, A = Na^+, K^+) phosphors

2003 J. Phys.: Condens. Matter 15 3471

(http://iopscience.iop.org/0953-8984/15/20/308)

INSTITUTE OF PHYSICS PUBLISHING JOURNAL OF PHYSICS: CONDENSED MATTER

J. Phys.: Condens. Matter **15** (2003) 3471–3480 PII: S0953-8984(03)56064-7

Luminescence and thermoluminescence of $Sr_2B_5O_9X:Ce^{3+}$, A^+ (X = Cl, Br, A = Na^+, K^+) phosphors

A V Sidorenko[1,4], A J J Bos[1], P Dorenbos[1], P A Rodnyi[2], C W E van Eijk[1], I V Berezovskaya[3] and V P Dotsenko[3]

[1] Interfaculty Reactor Institute, Delft University of Technology, Mekelweg 15, 2629 JB Delft, The Netherlands
[2] St Petersburg State Technical University, Polytekhnicheskaya 29, 195251 St Petersburg, Russian Federation
[3] A V Bogatsky Physico-Chemical Institute, Ukranian Academy of Science, 65080 Odessa, Ukraine

E-mail: asidore@iri.tudelft.nl

Received 14 November 2002
Published 12 May 2003
Online at stacks.iop.org/JPhysCM/15/3471

Abstract

The luminescence properties of Ce^{3+} activated strontium haloborates with and without K^+ or Na^+ co-doping have been studied under optical and x-ray excitation. Three types of Ce^{3+} emission centre have been found as the result of different methods of charge compensation in non-co-doped samples. In the co-doped compounds only one type of Ce^{3+} emission centre has been observed. The influence of Ce^{3+} concentration, anion type and co-doping ion on thermoluminescence (TL) has been analysed. The TL glow curves of all the studied materials contain two peaks. The emission corresponding to the low temperature peak is associated with charge uncompensated Ce^{3+} centres in non-co-doped compounds. The emission of the high temperature peak represents the superposition of both charge compensated and uncompensated Ce^{3+} centres. The emission corresponding to both TL peaks in co-doped samples originates from one type of Ce^{3+} centre.

1. Introduction

There is a growing interest in the development of low γ-ray sensitive storage phosphor materials for use in position sensitive thermal neutron detection. Haloborates represent promising materials for such applications [1]. Spectroscopic and storage properties of haloborates doped with Eu^{2+} have already been studied [2, 3]. Several disadvantages of Eu^{2+} doped haloborates

[4] Author to whom any correspondence should be addressed.

such as a low light yield and slow kinetics of photo-stimulated luminescence inspired us to study haloborates doped with other activators.

This work is a part of a more extensive work where the properties of haloborates for application in neutron imaging as a storage phosphor are investigated. Here we report on luminescence and thermoluminescence properties of haloborates doped with Ce^{3+}. The luminescence properties of $Sr_2B_5O_9Br:Ce^{3+}$ have been reviewed recently in [4]. In this paper an extended spectroscopic study of Ce^{3+} doped haloborates co-doped with monovalent cations is presented. The contributions of different Ce^{3+} centres in the TL spectra are discussed.

2. Experimental details

For the experiments several solid solutions of haloborates were synthesized in the A V Bogatsky Physico-Chemical Institute using the solid state method as described in [4]. The samples studied in this work are

(i) a series of non-co-doped $Sr_2B_5O_9Br$ and $Sr_2B_5O_9Cl$ samples with different concentrations of Ce^{3+} between 0.05 and 5 mol% and
(ii) several co-doped compounds: $Sr_{2(1-x)}Ce_xNa_xB_5O_9Br$ ($x = 0.01$ and 0.001), $Sr_{2(1-x)}Ce_xK_xB_5O_9Br$ ($x = 0.001$) and $Sr_{2(1-x)}Ce_xNa_xB_5O_9Cl$ ($x = 0.01$).

The given concentrations pertain to the starting materials. The powder samples were pressed into pills of 30 mg and 5 mm in diameter with an applied pressure of 125 kg mm^{-2}.

X-ray excited emission spectra were recorded using an x-ray tube with a Cu anode operated at 35 kV and 25 mA. The light emitted from the sample was detected by a combination of a vacuum monochromator (ARC VM502) and a PMT. Excitation/emission measurements in the UV and visible region were performed with a QuantaMaster QM-1 system from Photon Technology International. Excitation spectra around 10 K were performed at the Deutsche Electronen Synchrotron (DESY) in Hamburg (Germany) at the Superlumi station of Hasylab. The synchrotron operated in multibunch mode with bunches separated by 200 ns. The 'short time' excitation spectra were recorded after 1.5 ns delay in a 12 ns time gate. Time delayed excitation spectra were recorded after 74 ns delay in a 85 ns time gate. Excitation spectra at room temperature were recorded using our laboratory VUV spectrofluorometer. The detailed properties of this set-up have been described in [5].

For thermally stimulated luminescence measurements a Risø-TL/OSL-DA-15A/B reader was employed. A Sr^{90}/Y^{90} β-source installed in the reader with a dose rate of 1.0 mGy s^{-1} was used as irradiation source. For the measurements of emission spectra upon thermal stimulation, the PMT in the Risø reader was replaced by an optical fibre connected to a spectrophotometer. In that case a stronger irradiation source was required due to the lower sensitivity of the optical fibre and spectrophotometer. For this purpose a ^{60}Co γ-source with a dose rate of 0.7 kGy h^{-1} was used.

3. Results

3.1. Optical properties of Ce^{3+} in $Sr_2B_5O_9Br$ and $Sr_2B_5O_9Cl$.

Monovalent cations K^+ or Na^+ are commonly used co-dopants to provide charge compensation for trivalent rare-earth ions on divalent cation sites. Addition of monovalent cation increases the solubility of Ce_2O_3 in the borate matrix, which can lead to the increase of Ce^{3+} luminescence intensity. The emission spectrum of $Sr_{2(1-x)}Ce_xNa_xB_5O_9Br$ ($x = 0.01$) upon x-ray excitation results in a resolved Ce^{3+}emission doublet at 330 and 350 nm (figure 1, curve b). The

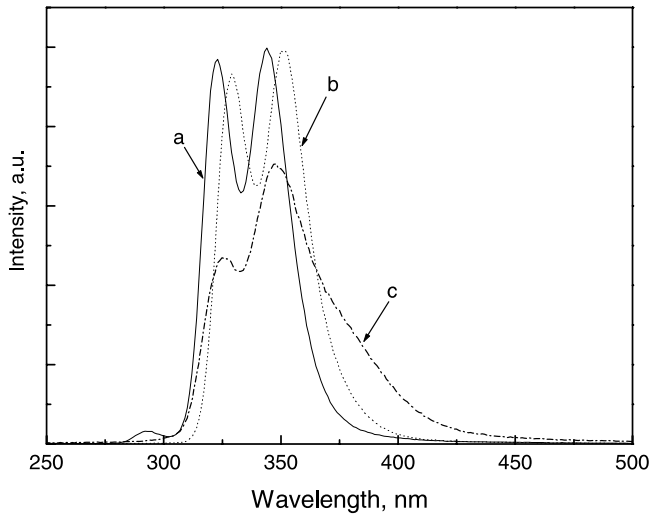

Figure 1. X-ray excited emission spectra of $Sr_{2(1-x)}Ce_xNa_xB_5O_9Cl$ ($x = 0.01$) (curve a), $Sr_{2(1-x)}Ce_xNa_xB_5O_9Br$ ($x = 0.01$) (curve b) and $Sr_{2(1-x)}B_5Ce_{2x}O_9Cl$ ($x = 0.01$) (curve c) recorded at room temperature.

replacement of bromine for chlorine leads to a shift of Ce^{3+} emission in $Sr_{2(1-x)}Ce_xNa_xB_5O_9Cl$ ($x = 0.01$) towards shorter wavelength (figure 1, curve a). The band in the emission spectrum of $Sr_{2(1-x)}Ce_xNa_xB_5O_9Cl$ ($x = 0.01$) (figure 1, curve a) between 280 and 303 nm might be due to SrB_4O_7 which is present in the sample as a phase impurity. The emission band due to the 5d-$^2F_{5/2}$ transition in Ce^{3+} in strontium tetraborate has a maximum at 293 nm [4].

The excitation spectra of Ce^{3+} emission in chlorides and bromides are shown in figure 2. The time resolved excitation spectrum of $Sr_{2(1-x)}Ce_xK_xB_5O_9Br$ ($x = 0.001$) emission at 350 nm has been recorded under synchrotron radiation at 12 K. In a short time excitation spectrum the five dominant bands with maxima at 223, 243, 268, 280 and 315 nm are attributed to the transitions to the five levels of the 5d Ce^{3+} configuration. In addition, two low intensity bands are located at 165 and 202 nm. The origin of the band at 165 nm (7.5 eV) can be attributed to the host excitation, since the typical bandgap energy of borates is about this value [6–8]. In the time delayed excitation spectrum the intensity of the band at 202 nm is dominant. This evidences that this band is not related to the 5d configuration of Ce^{3+}. The excitation spectrum of $Sr_{2(1-x)}Ce_xNa_xB_5O_9Cl$ ($x = 0.01$) has been recorded at room temperature using the VUV-spectrofluorometer. The excitation spectrum consists of the expected five bands of the 5d Ce^{3+} configuration with maxima at 219, 234, 270, 279 and 308 nm and two additional bands at 170 and 202 nm, see the inset of figure 2. The positions of the 5d excitation bands of Ce^{3+} in haloborates do not change whether K^+ or Na^+ is the monovalent co-dopant.

Various types of Ce^{3+} emission centre in compounds where Ce^{3+} substitutes for a divalent cation without additional co-dopants are expected due to different charge compensation mechanisms [9]. Excitation and emission spectra of Ce^{3+} in $Sr_{2(1-x)}Ce_{2x}B_5O_9Br$ ($x = 0.01$) are shown in figure 3. Two non-resolved emission bands at 330 and 352 nm observed under excitation at 315 nm are indicated as Ce_1^{3+} centre emission. This Ce_1^{3+} emission doublet is well resolved at 325 and 347 nm in the x-ray excited emission spectrum of $Sr_{2(1-x)}Ce_{2x}B_5O_9Cl$ ($x = 0.01$) (see curve c in figure 1). The position of the lowest 5d level of Ce_1^{3+} centres is the same as that of Ce^{3+} centres in co-doped compounds. Another broad emission band appears at about 375 nm under x-ray or photo-excitation and is indicated as Ce_2^{3+} centre emission

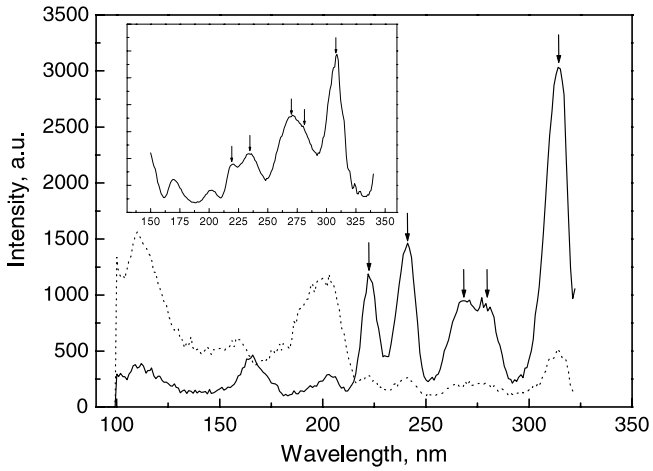

Figure 2. Excitation spectra of 350 nm emission of $Sr_{2(1-x)}Ce_xK_xB_5O_9Br$ ($x = 0.001$) recorded under synchrotron radiation at 12 K in a short time (solid curve) and time delayed (dotted curve). In the inset is the excitation spectrum of 350 nm emission of $Sr_{2(1-x)}Ce_xNa_xB_5O_9Cl$ ($x = 0.01$) recorded at room temperature. The arrows indicate the positions of Ce^{3+} 5d bands.

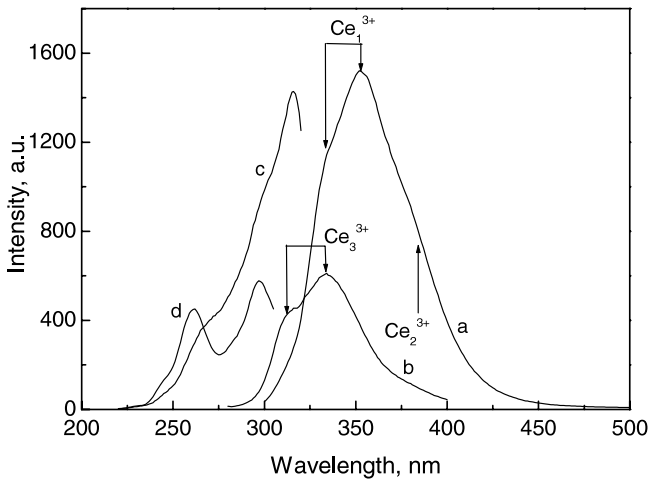

Figure 3. Emission spectra of $Sr_{2(1-x)}Ce_{2x}B_5O_9Br$ ($x = 0.01$) recorded at $\lambda = 315$ nm (curve a) and 260 nm (curve b) excitation. Excitation spectra of emission at $\lambda = 350$ nm (curve c) and 315 nm (curve d). All the spectra are recorded at room temperature.

in figure 3. The intensity of this long wavelength emission increases with increase of Ce^{3+} concentration. In the sample with 0.05 mol% of Ce^{3+} it has a very low intensity upon x-ray and photo-excitation at 315 nm, but the doublet at 330 and 352 nm is well resolved. It was not possible to resolve the 5d excitation bands of these Ce_2^{3+} centres with synchrotron radiation at 12 K.

Probable charge compensation mechanisms, which occur when a trivalent ion is introduced on a divalent site, can be performed by the creation of one vacancy at a strontium site per two Ce^{3+} ions or by an oxygen on a bromine site [4]. Usually Ce^{3+} centres with nearby charge compensators produce the emission at longer wavelength than isolated Ce^{3+} centres [10].

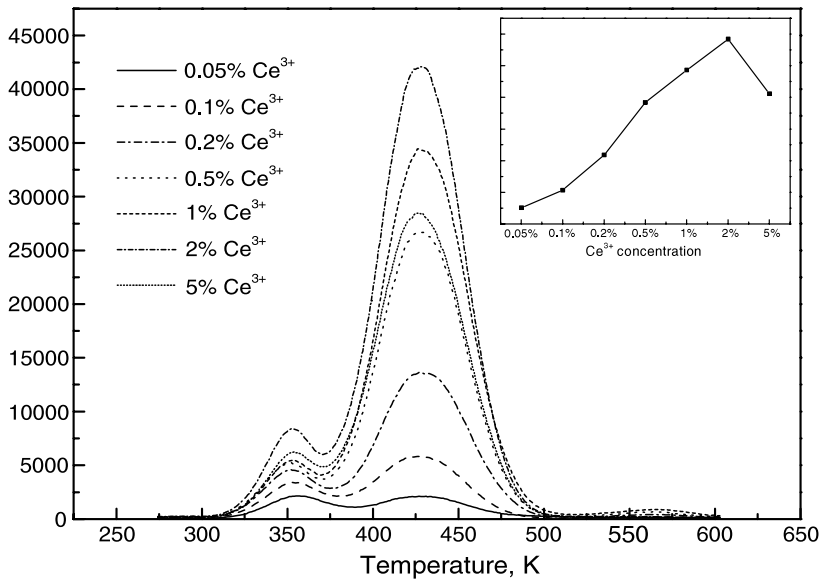

Figure 4. TL glow curves of $Sr_2B_5O_9Br:Ce^{3+}$ for different concentrations of Ce^{3+}. Heating rate is $\beta = 1$ K s^{-1}. In the inset the integral TL intensity as a function of Ce^{3+} concentration are plotted. The samples were irradiated for 30 s with a $^{90}Sr/^{90}Y$ β-source with the dose rate 1.0 mGy s^{-1}.

We therefore attribute the emission band at 375 nm to Ce^{3+} centres with nearby charge compensating defects.

A weak emission, see curve (b) in figure 3, with the resolved doublet at 315 and 334 nm has been detected at excitation with $\lambda = 260$ nm. This emission is associated with Ce_3^{3+} centres. This luminescence is not observed in all studied samples. When the sample showing the luminescence at 315 and 334 nm is fired in very dry nitrogen atmosphere at 500 °C for 1.5 h this luminescence disappears completely. This provides an argument that the luminescence at 315 and 334 nm is caused by Ce^{3+} centres associated with OH^- groups replacing the Br^- ions, i.e., this luminescence is a result of slow hydrolysis in air.

4. Thermoluminescence

The TL glow curves of $Sr_2B_5O_9Br$ with different concentrations of Ce^{3+} ions are shown in figure 4. For all Ce^{3+} concentrations there are two main TL glow peaks at 350 and 430 K and the positions of these peaks do not change with concentration. The integral intensity of the TL signal increases with increasing Ce^{3+} concentration up to 2 mol% as shown in the inset. The TL light yield of the $Sr_{2(1-x)}Ce_{2x}B_5O_9Cl$ ($x = 0.01$) sample is about four times more than that of the standard material TLD-100 [11]. The intensity ratio between the low and high temperature peaks changes with the Ce^{3+} concentration. The positions of both TL peaks do not change with absorbed radiation dose, which is consistent with a first order kinetics as described by the Randall–Wilkins equation [12]. Physically, it is a case of negligible retrapping of carriers during the thermal stimulation. However, a symmetrical shape of the peak at 430 K is not consistent with a first order kinetics. We could not fit this TL glow curve with several first order TL peaks.

The influence of monovalent cations, Na^+ or K^+, on TL glow curves of $Sr_2B_5O_9Br(Cl):Ce^{3+}$ is shown in figure 5. The TL intensity increases by a factor of approximately two when Na^+ is introduced. Monovalent co-dopants do not influence the shape

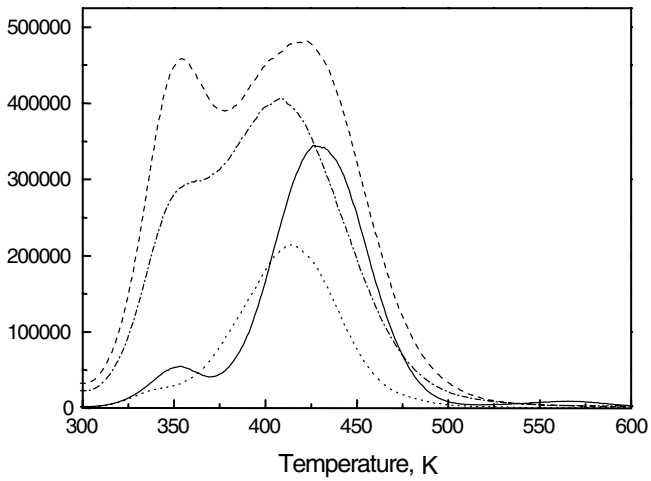

Figure 5. The TL glow curves of $Sr_{2(1-x)}Ce_{2x}B_5O_9Br$ ($x = 0.01$) (solid curve), $Sr_{2(1-x)}Ce_xNa_xB_5O_9Br$ ($x = 0.01$) (dashed curve), $Sr_{2(1-x)}Ce_{2x}B_5O_9Cl$ ($x = 0.01$) (dotted curve) and $Sr_{2(1-x)}Ce_xNa_xB_5O_9Cl$ ($x = 0.01$) (dashed–dotted curve) recorded with 1 K s^{-1} heating rate.

of the TL glow curve or the peak positions. However, the intensity of the low temperature peak relative to that at high temperature is much higher in the presence of co-dopants. If one compares the TL glow curves of bromides and chlorides, the position of the low temperature peak does not depend on the ligand anion (Cl^- or Br^-). The position of the high temperature peak is shifted towards lower temperature in the case of chlorides.

5. Emission spectra upon thermal stimulation

The structure of a TL glow curve gives the possibility to determine the characteristics of various traps. To establish the features of luminescence centres, the TL emission spectra should be measured. Emission spectra recorded at different temperatures during TL readout are shown in figure 6. Emission related to the TL peak at 350 K in $Sr_{2(1-x)}Ce_{2x}B_5O_9Br$ ($x = 0.01$) coincides with the emission of Ce_1^{3+} centres. But the emission related to the TL peak at 425 K is shifted towards longer wavelength and resembles the superposition of the emissions from Ce_1^{3+} and Ce_2^{3+} centres. The emission spectra of co-doped compounds measured near the low and high temperature TL peaks are very slightly different.

The TL emission as a function of the Ce^{3+} concentration and the type of co-dopant has been further investigated. TL measurements were performed with different band pass filters U-340 and HA-3. When the U-340 filter is placed between the sample and the PMT, the long wavelength emission of Ce_2^{3+} centres is absorbed. With the HA-3 filter all types of Ce^{3+} emission are transmitted. The ratio of TL signals measured with the two filters, i.e. TL_{HA-3}/TL_{U-340}, is a measure for the contribution of the long wavelength emission to the total TL signal. The results are listed in table 1. The ratio TL_{HA-3}/TL_{U-340} increases with increase of Ce^{3+} concentration. In compounds co-doped with Na^+ or K^+ the TL_{HA-3}/TL_{U-340} ratio is smaller than that for the sample with the same concentration of Ce^{3+} but without co-doping.

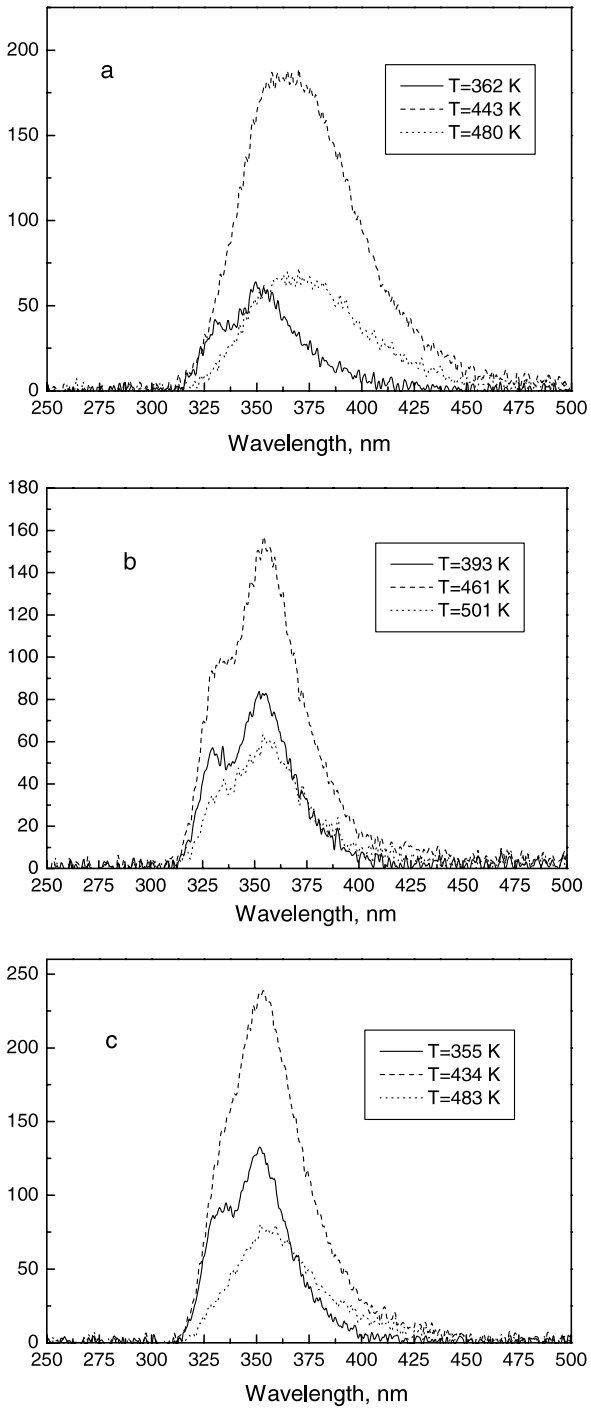

Figure 6. TL emission spectra of $Sr_{2(1-x)}Ce_{2x}B_5O_9Br$ ($x = 0.01$) (a), $Sr_{2(1-x)}Ce_xK_xB_5O_9Br$ ($x = 0.001$) (b) and $Sr_{2(1-x)}Ce_xNa_xB_5O_9Br$ ($x = 0.01$) (c). Measurements have been performed with 1 K s^{-1} heating rate after a received dose of 1 kGy with a ^{60}Co gamma source. The temperatures at which emission spectra have been taken are given.

6. Discussion

Crystallographic data on $Sr_2B_5O_9(Br, Cl)$ are not available, but there are data for $Eu_2B_5O_9(Br, Cl)$ [13]. There are two Eu^{2+} sites in this matrix; both of them are sevenfold coordinated by oxygen atoms with in addition two near halogen anions. Since Eu^{2+} and Sr^{2+} have the same ionic radii [14] we will assume that crystallographic data on europium haloborates are the same for strontium haloborates.

The two strontium sites in $Sr_2B_5O_9Br$ have very similar anion coordination polyhedra. In emission spectra in figure 1 and in excitation spectra of Ce^{3+} in figure 2 we could not distinguish two Ce^{3+} centres.

The relative positions of Ce^{3+} 5d levels are very similar in bromo- and chloroborates, as can be seen in figure 2. Since the relative positions of 5d levels are strongly determined by the shape and size of anion coordination polyhedra, this confirms that the polyhedral coordination of Ce^{3+} is practically the same in both compounds. The energy of the lowest 5d level in chloroborates is at 32 470 cm^{-1} against 31 4745 cm^{-1} for bromoborates. The difference of 720 cm^{-1} is practically the same as the difference between the average energy, i.e. centroid shift of the 5d configuration, which is 12 4480 cm^{-1} for $Sr_2B_5O_9Cl$ and 13 4115 cm^{-1} for $Sr_2B_5O_9Br$.

Morrison [15] and Aull and Jenssen [16] developed a model in order to explain the behaviour of the centroid shift of the 5d configuration of Ce^{3+} ions in fluorides. According to this model the shift is proportional to α/R^6, where α is the polarizability of the ligands and R is the metal–ligand distance. The ligand polarization model was further developed by Dorenbos in [17, 18] and applied to interpret the centroid shift in fluorides, chlorides, bromides and oxide compounds. Generally, a larger polarizability of bromine ions as compared to chlorine ions leads to larger centroid shift. If one takes the crystallographic data on strontium haloborates, the difference in mean strontium to oxygen distances in bromo- and chloroborates raised to the power six would be too small to explain the observed difference in centroid shift. But in a real situation there could be a significant difference in relaxation of ligands around a trivalent cerium ion substituted for a smaller divalent strontium ion in bromo- and chloroborates. Therefore, the observed difference in centroid shifts, which amounts to 720 cm^{-1}, appears to be too small to apply the ligand polarization model.

The formation of $(Ce_{Sr}\text{-}K_{Sr})$ complexes during the codoping was considered in [4]. The redshift of these Ce^{3+} centres is the same as that of charge uncompensated Ce^{3+} ions in compounds without co-doping, i.e. Ce_1^{3+} centres. Either the effect of a nearby K^+ is very small or it is placed in a next neighbouring Sr site.

The Ce^{3+} emission doublet at 315 and 334 nm detected in $Sr_2B_5O_9Br$, see figure 3, was assumed to originate from Ce^{3+} with nearby OH groups in a halogen site. The shift of this Ce_3^{3+} emission towards shorter wavelength is consistent with the ligand polarization model, since polarizability of OH groups is smaller than that of Br or Cl ions and thus the centroid shift of Ce_3^{3+} levels is expected to be smaller [18]. However, the 5d configuration of Ce_3^{3+} centres must be known to base this conclusion more firmly.

In some compounds like SrB_4O_7 and $CaSO_4$ two different Ce^{3+} emission centres have been found [10, 19]. Centres with the largest redshift were attributed to Ce^{3+} ions with nearby charge compensation. Another possibility for charge compensation in $Sr_2B_5O_9(Br, Cl):Ce^{3+}$ can be an oxygen in a bromine site next to Ce^{3+}. In this case the higher intensity of the long wavelength emission for the sample synthesized in air than in nitrogen atmosphere is expected. But the emission at 375 nm of the $Sr_2B_5O_9Br$:0.3%Ce^{3+} sample synthesized in air has lower intensity than that of $Sr_2B_5O_9Br$:1%Ce^{3+} synthesized in nitrogen atmosphere. The fact that it was not possible to resolve the 5d-excitation bands of these Ce_2^{3+} centres upon synchrotron

Table 1. Integral intensity of TL signal and its dependence on the filter used. For detailed information see the text.

Compound	Concentration (%)	TL intensity HA-3	TL intensity U-340	TL_{HA-3}/TL_{U-340}
$Sr_2B_5O_9Br:Ce^{3+}$	0.05	2.6	1.3	1.9
	0.1	5.3	2.3	2.3
	0.2	10.9	4.3	2.5
	0.5	19.2	6.0	3.2
	1	24.3	6.5	3.8
	2	29.2	5.6	5.2
	5	20.6	3.6	5.7
$Sr_2B_5O_9Br:Ce^{3+}$, Na^+	0.1, 0.1	20.5	8.1	2.5
	1, 1	61.5	23.0	2.7
$Sr_2B_5O_9Br:Ce^{3+}$, K^+	0.1, 0.1	55.6	25.3	2.2

radiation at 12 K indicates that several Ce^{3+} centres are responsible for the emission at 375 nm. Consequently, several charge compensation mechanisms can occur in $Sr_2B_5O_9(Br, Cl):Ce^{3+}$.

The probability that a charge compensating defect is placed near a Ce^{3+} site becomes higher with the increase of Ce^{3+} concentration. The assumption that the emission at 330 and 350 nm is caused by Ce_1^{3+} ions without nearby charge compensators then seems to be reasonable, since this emission is dominant upon x-ray and optical excitation of Ce^{3+} doped samples with very low concentrations (0.05% and less). X-ray and optically excited emission measurements show that the contribution to the total light output from long wavelength emission, i.e. Ce_2^{3+} centres with nearby charge compensation, increases with the concentration of Ce^{3+} ions.

Two types of Ce^{3+} emission centre have been detected in TL emission spectra of $Sr_2B_5O_9Br:Ce^{3+}$. Only the emission from Ce_1^{3+} centres, i.e. locally uncompensated Ce^{3+} ions, gives rise to the TL peak at 350 K. Probably, upon irradiation the Ce_1^{3+} centres are involved in charge trapping or it occurs in their vicinity. The emission spectrum corresponding to the second TL peak at 430 K is the superposition of two types of Ce_1^{3+} and Ce_2^{3+} emission. It is seen in figure 4 that the intensity of this glow peak increases significantly with concentration of Ce^{3+}. Also the contribution to TL signal from Ce_2^{3+} centres grows with Ce^{3+} concentration (see table 1), which is the result of a larger number of Ce_2^{3+} centres than of Ce_1^{3+} centres at high concentrations. We conclude that the defects responsible for the high temperature peak are not connected with the charge compensation mechanism for Ce^{3+}, but belong to the internal properties of the haloborate matrix.

7. Conclusion

Two types of Ce^{3+} centre have been detected in $Sr_2B_5O_9(Br, Cl):Ce^{3+}$ and they can be associated with isolated Ce_1^{3+} and charge compensated Ce_2^{3+} centres. Probably, several charge compensation defects are responsible for the Ce_2^{3+} emission. Only one type of Ce^{3+} emission centre was detected in the samples co-doped with Na^+ or K^+. The emission is the same as that of the isolated Ce_1^{3+} centres. Two peaks appear in TL glow curves at 350 and 430 K for both co-doped and non-co-doped samples. The relative intensity of the peak at 350 K is higher in the case of co-doping. Also the integral TL intensity doubles when monovalent cations are introduced. The TL emission of $Sr_2B_5O_9(Br, Cl):Ce^{3+}$ related to the low temperature peak originates from (Ce_1^{3+}) centres. The emission in the 430 K peak is from both Ce_1^{3+} and Ce_2^{3+} centres. The TL emission corresponding to both TL peaks in co-doped samples originates from the single type of Ce^{3+} centre.

Acknowledgments

This investigation was supported by the Netherlands Technology Foundation (STW) and by the IHP contract HPRI-CT-1990-00040 of the European Commission.

References

[1] Knitel M J, Bom V R, Dorenbos P, van Eijk C W E, Berezovskaya I V and Dotsenko V P 2000 *Nucl. Instrum. Methods* A **449** 595
[2] Knitel M J 1998 New inorganic scintillators and storage phosphors for detection of thermal neutrons *PhD Thesis* Delft University of Technology
[3] Meijerink A and Blasse G 1989 *J. Lumin.* **43** 283
[4] Dotsenko V P, Berezovskaya I V, Efryushina N P, Voloshinovskii A S, Dorenbos P and van Eijk C W E 2001 *J. Lumin.* **93** 137
[5] van der Kolk E 2001 Photon cascade emission of Pr^{3+} and optimization of Mn^{2+} based phosphors *PhD Thesis* Delft University of Technology
[6] French R H, Ling J W, Ohuchi F S and Chen C T 1991 *Phys. Rev.* B **44** 8496
[7] Efryushina N P, Dotsenko V P, Berezovskaya I V and Ryzhkov M V 2001 *Radiat. Meas.* **33** 755
[8] Knitel M J, Dorenbos P, van Eijk C W E, Plasteig B, Viana B, Kahn Harari A and Vivien D 2000 *Nucl. Instrum. Methods* A **443** 364
[9] Hayes W (ed) 1974 *Crystal with the Fluorite Structure* (Oxford: Clarendon)
[10] Verwey J W M, Dirksen G J and Blasse G 1992 *J. Phys. Chem. Solids* **53** 367–75
[11] Hommels L B A 1998 *Interfaculty Reactor Institute Report* ST-ISO-980095 (unpublished)
[12] Chen R and McKeever S W S 1997 *Theory of Thermoluminescence and Related Phenomena* (Singapore: World Scientific)
[13] Machida K, Ishino T, Adachi G and Shiokawa J 1979 *Mater. Res. Bull.* **14** 1529
[14] Shannon R D 1976 *Acta Crystallogr.* A **32** 751
[15] Morrison C A 1980 *J. Chem. Phys.* **72** 1001
[16] Aull B F and Jenssen H J 1986 *Phys. Rev.* B **34** 6640
[17] Dorenbos P 2000 *Phys. Rev.* B **62** 15640
[18] Dorenbos P 2001 *Phys. Rev.* B **65** 125117
[19] van der Kolk E, Dorenbos P, Vink A P, Perego R C, van Eijk C W E and Lakshmanan A R 2001 *Phys. Rev.* B **64** 195129